Journal of Mining and Earth Sciences

Website: https://jmes.humg.edu.vn

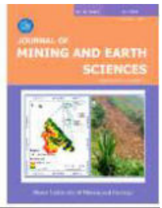

Landslide hazard assessment for the Batxat area of Vietnam using GIS-based spatial prediction models

Binh Van Duong[1,*], Igor Konstantinovich Fomenko[2], Ha Viet Nhu[1], Phuong Huy Nguyen[3], Olga Nikolaevna Sirotkina[4], Kien Trung Nguyen[5], Ha Ngoc Thi Pham[1]

[1] *Hanoi University of Mining and Geology, Hanoi, Vietnam*
[2] *Sergo Ordzhonikidze Russian State Geological Prospecting University, Moscow, Russia*
[3] *Vietnam Association of Engineering Geology and Environment, Hanoi, Vietnam*
[4] *Lomonosov Moscow State University, Moscow, Russia*
[5] *Institute of Geological Sciences - Vietnam Academy of Science and Technology, Hanoi, Vietnam*

ARTICLE INFO

Article history:
Received 25th Apr. 2024
Revised 17th Aug. 2024
Accepted 9th Sept. 2024

Keywords:
Analytic Hierarchy Process,
Batxat,
Frequency Ratio,
GIS,
Landslide hazard.

ABSTRACT

Located in the northwest of Laocai province, Batxat district has been frequently affected by natural disasters, including landslides and debris flows. Therefore, landslide hazard assessment (LHA) has been a significant task for planning, economic development, and minimizing human and property damage. For this purpose, landslide hazard maps were established in this study using the Analytic Hierarchy Process (AHP) and the combined Analytic Hierarchy Process - Frequency Ratio (AHP&FR) models. Ten landslide-related factors were selected, including elevation, slope, distance to road, distance to drainage, land use and land cover (LULC), average monthly rainfall, lithology, aspect, distance to fault, and relative relief. Afterwards, the weighted value of landslide-related factors and the landslide susceptibility index (LSI) were determined using the Analytic Hierarchy Process. The Frequency Ratio method was used to calculate the weighted value of factor classes. Two landslide hazard maps were established, and the study area was divided into five hazard zones: very low, low, moderate, high, and very high. The performance of the models was determined using the area under the curve (AUC) of the receiver operating characteristic (ROC), the seed cell area index (SCAI), and the precision of the predicted results (P). The AUC values for the success rate of these models were 0.72 and 0.75, and for the prediction rate were 0.67 and 0.70, respectively. The evaluation results of the models showed that, although both the AHP and combined AHP&FR models have good performance for landslide hazard mapping, the AHP&FR model produces more accurate outcomes than the AHP model.

*Corresponding author
E - mail: duongvanbinh@humg.edu.vn
DOI: 10.46326/JMES.2022.65(6).07

1. Introduction

Landslide is one of the most devastating natural disasters that occurs worldwide, causing significant damage to people and property (Althuwaynee et al., 2012; Mandal & Mondal, 2019; Nguyen et al., 2021; Tran et al., 2021). Their occurrence is attributed to the Earth's geological environment and meteorological processes (Ma et al., 2021). Landslides are frequently caused by geologic, geographic, or climatic factors that are common in large areas. Landslide causes and triggers include slope-related factors that may increase shear stresses and reduce shear strength (Varnes, 1978). Therefore, knowing the mechanisms of landslides and landslide hazard mapping (LHM) is important and may be regarded as a standard tool to assist decision-making activities (Bui et al., 2016).

Landslide susceptibility, landslide hazard, and landslide risk are the three fundamental components of the landslide study (Shano et al., 2020). Landslide susceptibility mapping (LSM) is the process of determining the spatial distribution and classifying terrain units based on their tendency to generate landslides. A landslide susceptibility map is the basis for establishing a landslide hazard map, which indicates the likelihood of landslide events throughout a particular period and in a specific area (Varnes et al., 1984).

Recently, numerous GIS-based models and approaches have been used by scientists to evaluate landslide hazards and generate hazard maps depicting their spatial distribution (Akgun & Türk, 2010; Vahidnia et al., 2009). In general, these models can be classified into three groups: 1) heuristic, 2) deterministic, and 3) statistical methods (Dou et al., 2019). In landslide studies, various decision-making support tools for GIS-based heuristic analysis methods, including the Analytical hierarchy process (AHP), have been developed (Akgun & Türk, 2010). The AHP (Saaty, 1977, 1990, 2008) is a decision-making method that was originally suggested and developed by Saaty. Its primary purpose is to provide solutions to decision-making and estimating issues in multivariate environments. There are many bivariate statistical approaches for mapping landslide susceptibility, of which the Frequency ratio (FR) method is one of the most frequently used (Shano et al., 2021).

In landslide studies, the AHP and FR have been used by many authors all over the world, including those in Vietnam for LHM (Dang et al., 2020; Le et al., 2021; Senouci et al., 2021; Shano et al., 2021). Additionally, the AHP has been combined with other methods to improve the effectiveness of LHA (Mokarram & Zarei, 2018; Zhang et al., 2016). In this study, the AHP and the combined AHP&FR models were employed for LHM in Batxat, Laocai. In comparison with the AHP, the FR considers the correlation between the locations of historical landslides and the related factors, so this approach can improve the performance of the landslide prediction. To evaluate the performance of the models, the landslide susceptibility maps and landslide hazard maps were compared with the landslide inventory map using the area under the curve (AUC) of the receiver operating characteristic (ROC), the seed cell area index (SCAI), and the precision of the predicted results (P) values.

2. Materials and methods

2.1. Study area

Batxat is a district in the Northwest Vietnam mountainous region, which is known as one of the most landslide-prone regions in the country (Bui et al., 2017) (Figure 1a). Some landslide events were recorded in the study, such as a landslide in Phin Ngan commune (2004) that killed 23 people (Figure 1b), medium-sized landslides in Muong Hum commune (2013), Phin Ngan (2020). Landslides in the Northwest Vietnam region are caused by eight main factors that are (Nguyen & Dao, 2007): 1) Relief slope: Landslides often occur at slopes greater than 25^0 (most frequently between 30^0 and 45^0); 2) weathering process of rocks: Numerous landslides with a sliding surface at the interface between the original rocks and the incomplete weathering zone (Tran et al., 2019); 3) Modem present tectonic movement; 4) Hydro-system: Landslides often occur in regions with heavy rainfall, and throughout the rainy season; 5) Vegetation density: Landslides occur most often and strongly in areas with little plant cover;

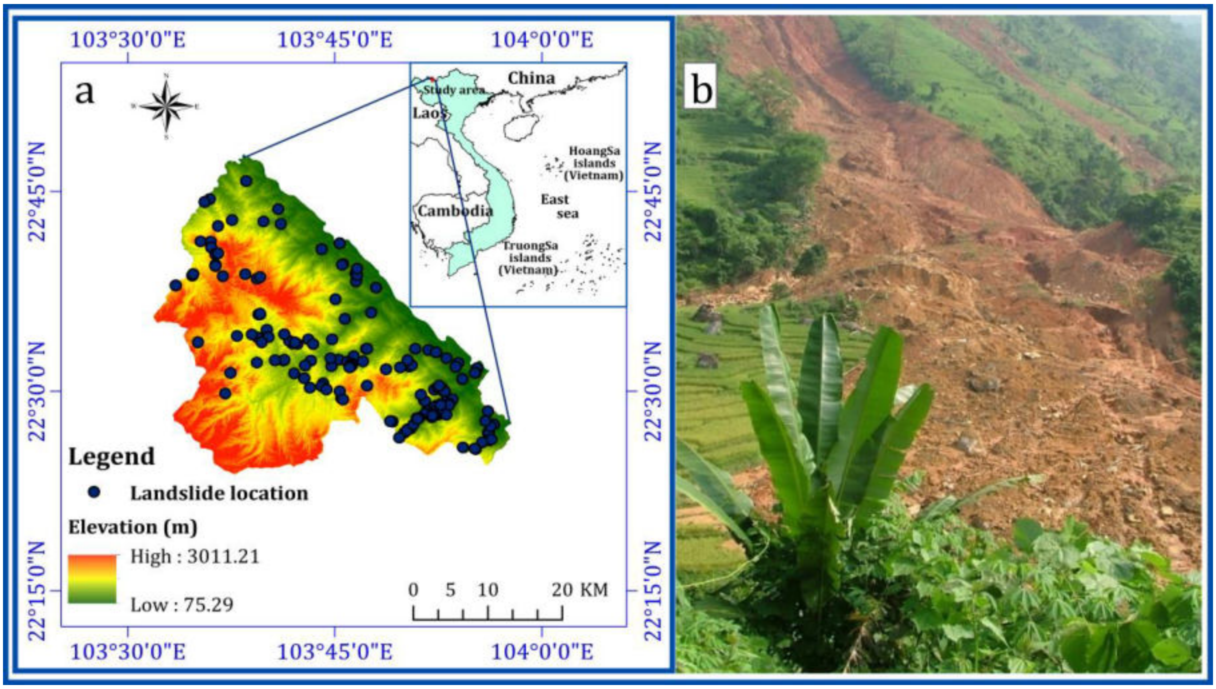

Figure 1. Location of study area (a) and photo of a landslide in Phin Ngan commune (b).

6) Striking and dipping of original rocks: Numerous landslides occur in locations where the relief slope direction coincides with the dipping or foliation of original rocks; 7) Physical property and structure of original rocks: Landslides often occur in weakening and severely broken-up rock zones; 8) Human activity that may trigger a landslide directly or indirectly. The study area has numerous geological formations that may be divided into three groups: 1) Shales, sandstones, and siltstones (SSS); 2) Quartz-biotite schists, graphite schists, and amphibolites (QGA); 3) Granodiorite, granite, and granite-migmatite (GGM). The total annual rainfall in the study region ranges from 2,000 to 3,600 mm due to its location in the high rainfall zone of the Hoang Lien Son mountain range (Bui et al., 2017).

2.2. Analytic Hierarchy Process (AHP)

In the AHP method (Saaty, 1990, 2008; Saaty & Vargas, 2001), the landslide susceptibility map of the study area could be prepared by utilizing class weights and factor weights with a reasonable consistency ratio (CR).

The Consistency Ratio (CR) is the ratio of the consistency index (CI) to the average consistency index (RI) for the same order matrix (Saaty, 2002). The consistency index (CI) is calculated using the following formula (Saaty, 1990, 2002):

$$CI = \frac{\lambda_{max} - n}{n - 1} \qquad (1)$$

Where λ_{max} - the largest eigenvalue and n – the order of the matrix. If the consistency ratio (CR) is less than 10%, the weight estimate (W) is considered appropriate (Saaty, 1990). As a final step, all of the weights of the classes and factors are integrated into a single landslide susceptibility index (LSI) (Cantarino et al., 2019):

$$LSI = \sum_{j=1}^{n} W_j . X_{ij} \qquad (2)$$

Where W_j - the weight of factor j, X_{ij} - the weight of class i of factor j, and n - the number of factors.

2.3. Frequency ratio method (FR)

The FR method has been widely and effectively applied in various studies for LSM (Gholami et al., 2019; Shano et al., 2021). Based on the analysis of relationships between the distribution of landslides and each landslide-related factor, the frequency ratio approach determines the correlation between the locations of landslides and these factors in the study area. As a result, the frequency ratio values for each factor were calculated based on their association with landslides (Yalcin et al., 2011). The frequency ratio of each range/class of all landslide-related factors is summed together to get the LSI (Mandal & Mondal, 2019; Shano et al., 2020):

$$LSI = \sum Fr \qquad (3)$$

Where LSI – landslide susceptibility index; Fr – frequency ratio/rating for each class/range of landslide-related factor.

2.4. Landslide inventory map

Actual landslide mapping in the study area is critical for defining the connection between the landslide distribution and the influencing variables (Pourghasemi et al., 2013). The landslide inventory maps have been used to assign or compute rating values for landslide-related factors and validate analysis results. In the study area, a total of 156 landslide sites were identified and mapped, with the largest landslide covering an area of about 20896.06 m^2 and the smallest covering an area of approximately 917.65 m^2. The training and testing data sets were prepared using 70% and 30% of the landslide locations, respectively.

2.5. Landslide-related factors

The landslide-related factors are considered to depend on the features of landslides, data available, and the connection with historical landslides. In this study, rainfall is the main landslide triggering factor, and most landslides occurred along the roads. In addition, the set of factors has been selected in previous studies for LSM (Bui et al., 2017; Le et al., 2021). Therefore, ten landslide-related factors were selected for LSM and LHM: Elevation, slope, distance to road, distance to drainage, land use and land cover (LULC), rainfall, lithology, aspect, distance to faults, and relative relief (Figure 3). Two estimators, "Accountability" (A) and "Reliability" (R), were used in this study to determine the importance of the factors causing landslide occurrences (Greenbaum et al., 1995a; Greenbaum et al., 1995b). The class weights of these factors were determined using the AHP and FR methods. The factor weights were determined using the AHP method (Table 1).

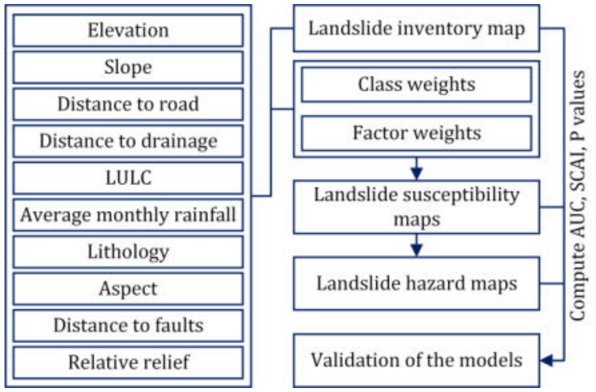

Figure 2. Flow chat of LHA.

2.6. Validation of the landslide susceptibility map

The validation was produced by comparing the landslide susceptibility and landslide hazard maps to the landslide inventory map. In this study, the AUC, SCAI, and P values were used for evaluating the performance of the models. The AUC value ranges between 0.5 and 1.0 (Cantarino et al., 2019) and is divided into six categories (Šimundić, 2009). The SCAI value, which indicates the density of landslides within each class, is calculated as the ratio of the area (%) of each landslide hazard class to the area (%) of landslides within each class (Süzen & Doyuran, 2004). The P value is calculated by the ratio of the area covered by landslides in the upper-moderate landslide hazard class (K_S) to the total area covered by landslides (S) in the study area (Mokhtari & Abedian, 2019).

3. Results

Figure 2 represents the process of landslide hazard assessment performed in this study. According to the data analysis, LULC and Distance to road play the most significant role in landslide occurrences. The LSI was calculated using formula (2) and two landslide susceptibility maps were established in GIS (Figure 4). The calculated LSI value, which ranged between 0.12 and 0.48 (AHP model), and 0.07 and 0.45 (combined AHP&FR model), was categorized into five landslide hazard classes: very low, low, moderate, high, and very high (Figure 5).

Table 1. Weights of classes and factors using AHP and FR.

Factor	Class	% Area	Landslide	A	R	Class weight			Factor weight (W_j)
						AHP		FR	
						X_{ij}	CR	FR	
Elevation (m)	< 500	23.32	54	76.85	8.51	0.429	0.027	2.124	0.112
	500÷1000	24.15	31			0.278		1.178	
	1000÷1500	21.70	19			0.184		0.803	
	1500÷2000	18.50	5			0.065		0.248	
	> 2000	12.34	0			0.044		0	
Slope (Degree)	< 15	13.25	17	44.24	6.14	0.124	0.04	1.177	0.103
	15÷25	24.62	36			0.343		1.342	
	25÷35	33.87	32			0.335		0.867	
	35÷45	21.6	22			0.158		0.934	
	> 45	6.66	2			0.04		0.276	
Distance to road (m)	< 500	48.60	91	80.38	8.69	0.55	0.039	1.718	0.209
	500÷1000	20.13	15			0.24		0.684	
	1000÷1500	10.21	2			0.082		0.179	
	1500÷2000	5.83	0			0.051		0	
	> 2000	15.23	1			0.077		0.06	
Distance to drainage (m)	< 250	28.55	49	74.04	7.18	0.531	0.031	1.574	0.102
	250÷500	25.62	29			0.118		1.039	
	500÷750	21.91	22			0.192		0.921	
	750÷1000	16.52	7			0.118		0.389	
	> 1000	7.41	2			0.04		0.247	
LULC	Water	0.42	0	44.37	16.84	0.044	0.018	0	0.181
	Forest	79.64	62			0.487		0.714	
	Agriculture	6.1	5			0.071		0.752	
	Shrub	11.18	28			0.232		2.298	
	Build area	1.56	12			0.122		7.058	
	Bare land	1.09	2			0.045		1.679	
Average monthly rainfall (mm/mth)	< 250	33.76	27	56.70	7.20	0.348	0.021	0.734	0.062
	250÷280	26.94	29			0.492		0.988	
	280÷310	24.89	25			0.072		0.922	
	310÷350	9.85	19			0.044		1.77	
	> 350	4.56	9			0.044		1.811	
Lithology	SSS	14.52	25	67.7	5.81	0.143	0	1.58	0.107
	GGM	46.67	51			0.571		1.003	
	QGA	38.81	33			0.286		0.78	
Aspect	Flat	0.18	0	72.97	6.78	0.02	0.021	0	0.027
	North	8.13	11			0.088		1.241	
	Northeast	17.56	13			0.111		0.679	
	East	16.48	17			0.196		0.947	
	Southeast	11.25	10			0.077		0.815	
	South	9.52	15			0.144		1.445	
	Southwest	8.88	15			0.144		1.55	
	West	9.26	7			0.053		0.693	
	Northwest	11.51	12			0.1		0.957	
	North	7.25	9			0.067		1.139	
Distance to faults (m)	< 900	48.71	54	98.59	5.87	0.437	0.026	1.017	0.048
	900÷2200	27.6	33			0.286		1.097	
	2200÷4200	11.86	18			0.171		1.392	
	4200÷6500	7.04	2			0.06		0.26	
	> 6500	4.79	2			0.045		0.382	
Relative relief (m/km^2)	< 250	12.23	10	73.12	6.74	0.088	0.037	0.75	0.05
	250÷400	29.02	44			0.442		1.391	
	400÷520	27.97	37			0.297		1.213	
	520÷650	23.3	16			0.126		0.63	
	> 650	7.48	2			0.048		0.245	

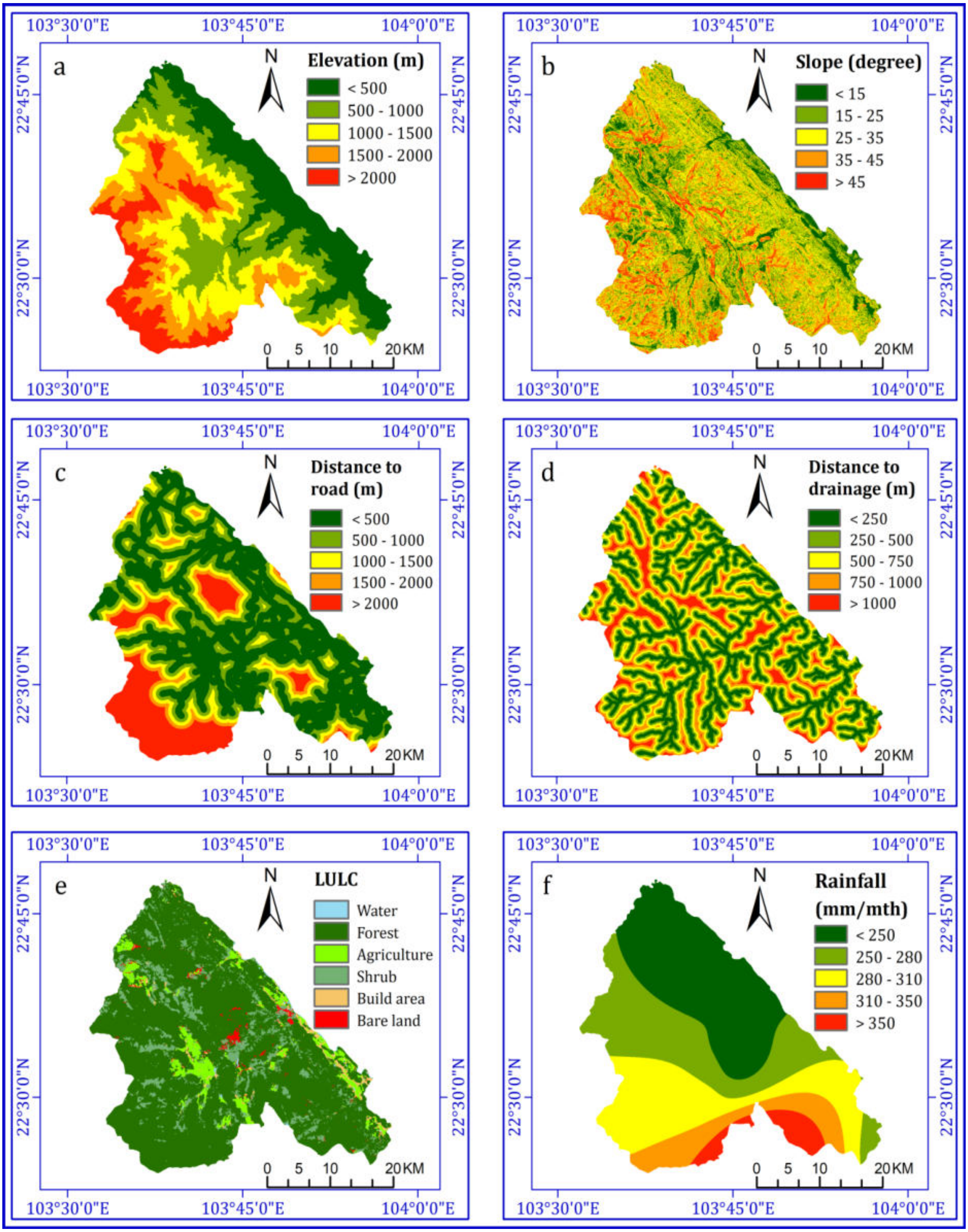

Figure 3. Landslide-related factors maps: (a) elevation, (b) slope, (c) distance to road, (d) distance to drainage, (e) LULC, (f) rainfall, (g) lithology, (h) aspect, (i) distance to faults, and (j) Relative relief.

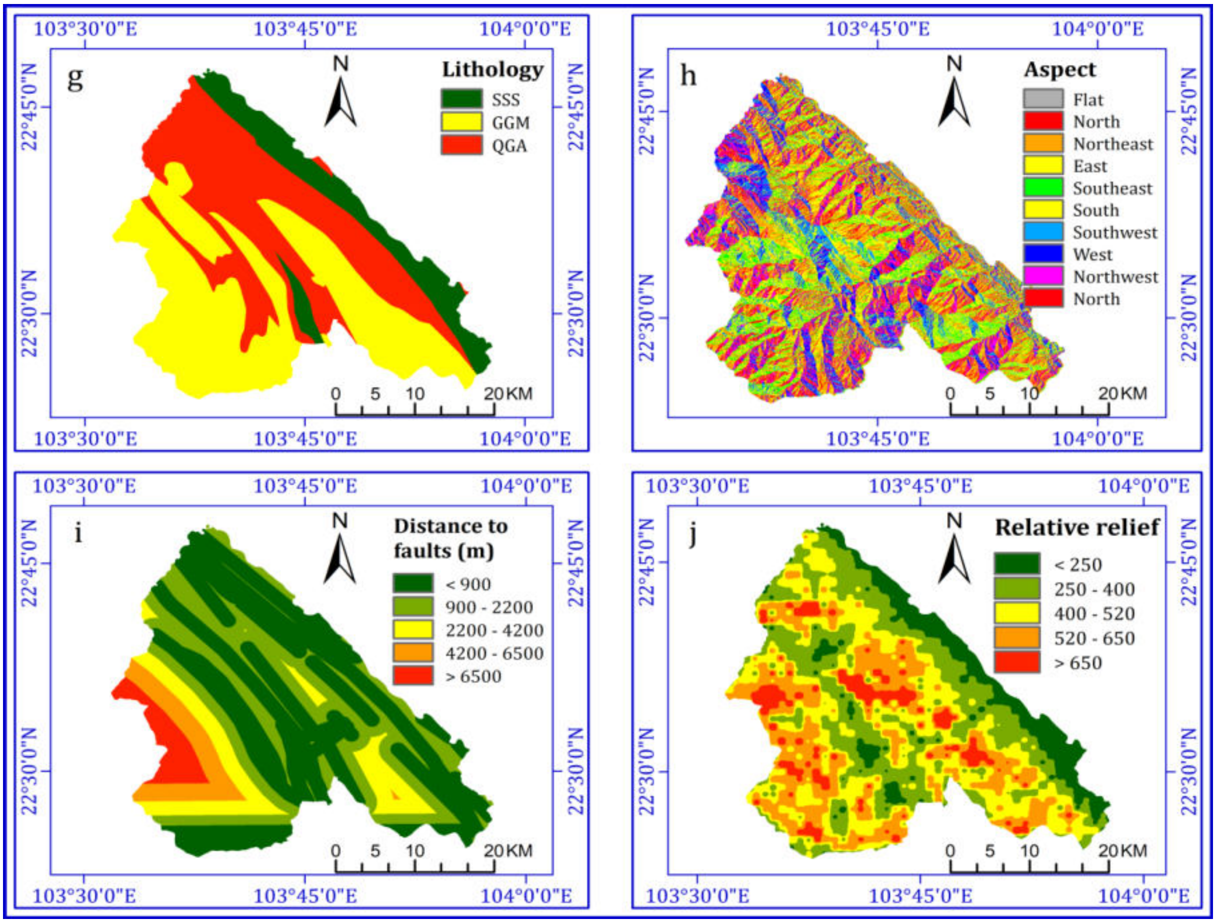

Figure 3 (Continued).

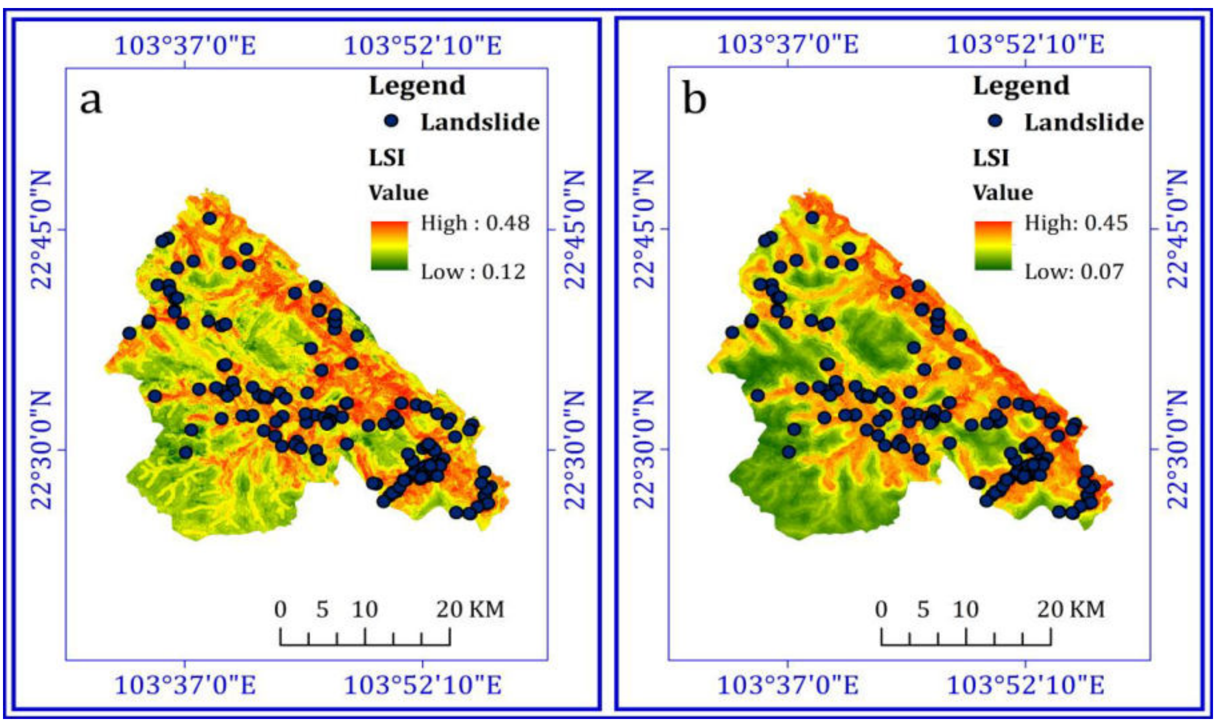

Figure 4. Landslide susceptibility maps using AHP (a) and combined AHP&FR (b) methods.

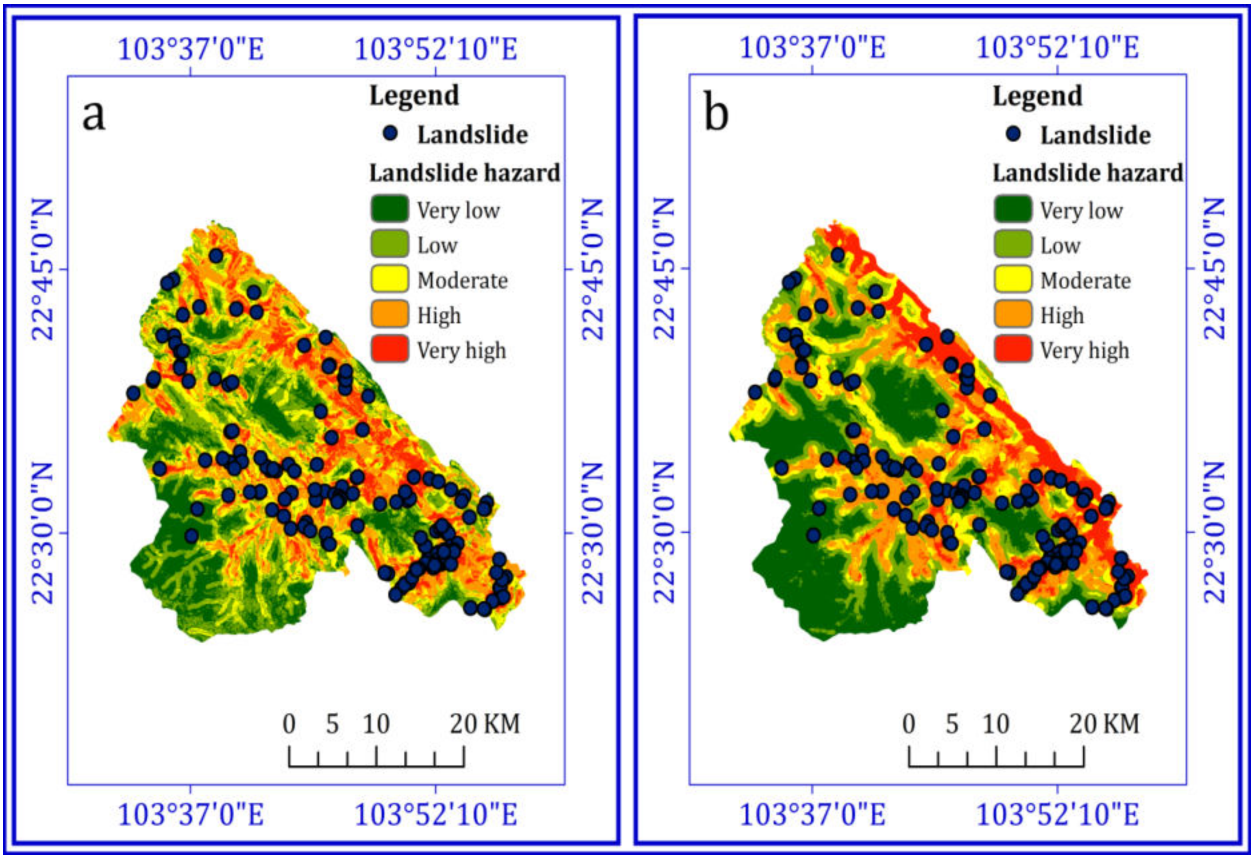

Figure 5. Landslide hazard maps using AHP (a) and combined AHP&FR (b) methods.

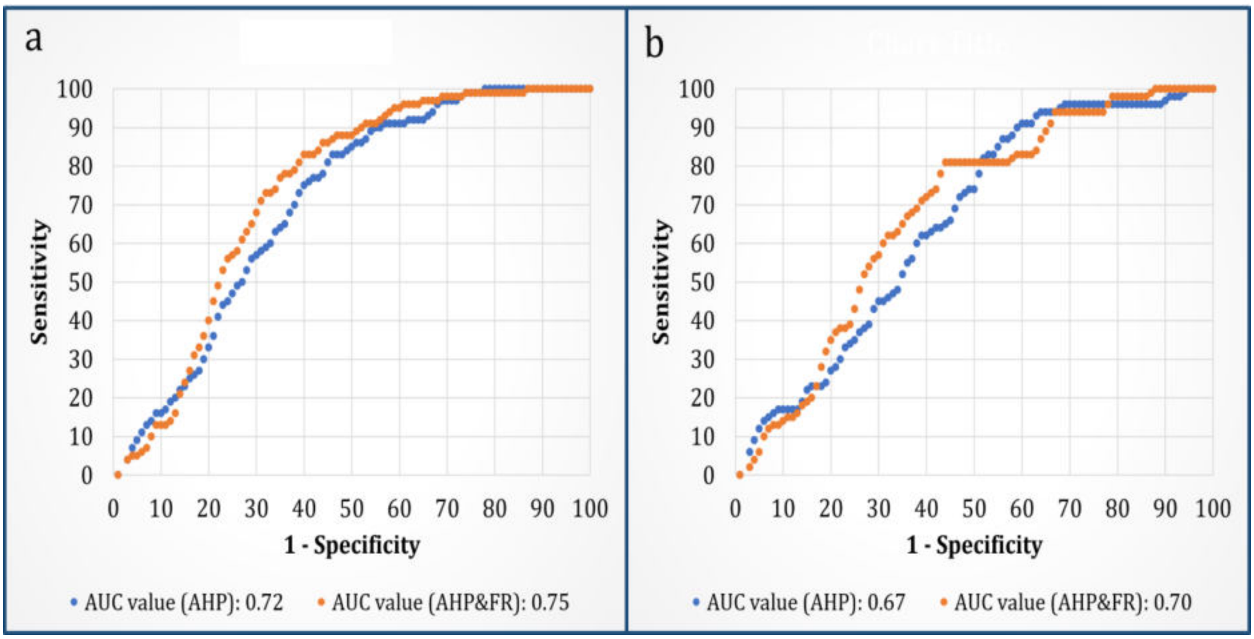

Figure 6. Performance of the landslide susceptibility assessment using AHP and combined AHP&FR methods (a – Success rate and b – Prediction rate).

Table 2. Accuracy and Precision of the predicted results using SCAI and P.

Method	Class	% Area	% Landslide area	SCAI	K_S (km^2)	S (km^2)	P (%)
AHP	Very low	17.59	5.16	3.41	2.85	55.2	57.35
	Low	23.22	13.19	1.76	7.28		
	Moderate	21.59	24.29	0.89	13.41		
	High	24.41	32.61	0.75	18.00		
	Very high	13.19	24.75	0.53	13.66		
Combined AHP&FR	Very low	26.61	2.43	10.95	1.34	55.2	75.09
	Low	18.64	7.07	2.64	3.9		
	Moderate	14.19	15.42	0.92	8.51		
	High	24.2	28.46	0.85	15.71		
	Very high	16.36	46.63	0.35	25.74		

According to AHP analysis, very low, low, moderate, high, and very high hazards account for 17.59%, 23.22%, 21.59%, 24.41%, and 13.19%, respectively, of the study area. Similarly, based on the results of the combined AHP&FR analysis, the assessment determined that 26.61%, 18.64%, 14.19%, 24.20%, and 16.36% of the study area, respectively, are in very low, low, moderate, high, and very high landslide hazard areas (Table 2). According to the AHP and combined AHP&FR models, 38 and 76 of the total landslide locations, correspondingly, are in the very high landslide susceptible area. The performance of the methods was evaluated using AUC, SCAI, and P values. The AUC values for the success rate of the AHP and combined AHP&FR models are 0.72 and 0.75, and for the prediction rate are 0.67 and 0.70, respectively. The precisions of the predicted outcomes by the AHP and combined AHP&FR models are 57.35% and 75.09%, respectively. The results are shown in Figure 6 and Table 2.

4. Discussion

This study demonstrated the effectiveness of the AHP method in landslide hazard assessment. The analysis results of the two models are acceptable, and both models are appropriate for assessing landslide susceptibility in the study area. By combining the AHP and FR methods, the performance of the analysis model was improved. This is demonstrated by the results of the accuracy evaluation using the AUC and SCAI values. Using the SCAI value, the accuracy of the models is higher when the SCAI value is higher in the very low hazard class and very low in the very high hazard class. As shown in Table 2, the combined AHP&FR model performs better in the very low and very high hazard zones. The AHP performance is better only in moderate and high-hazard zones. The very low and very high hazard zones are especially significant since they are directly linked to land use and long-term planning. According to the combined AHP&FR model, the very low hazard zone accounts for 26.61% of the study area, compared to 17.59% in the AHP model. In addition to improving the flexibility of land use planning in the study area, this shows the predictive performance of the models. This may be explained by the fact that the AHP model calculates the rating values of the classes and factors mostly based on expert opinion, which may lead to an underestimate of the influence of factors affecting the occurrence of landslides. Because of this disadvantage, the AHP has combined with other models to improve the performance of landslide prediction (Akgun & Türk, 2010; Mokarram & Zarei, 2018). Additionally, the combined AHP&FR model calculated rating values for the factor classes using the training data, thus improving the correlation between the factors and the landslide locations in the study area. The results show that Distance to road and LULC have the strongest influence on the landslide process in the study area. However, expert opinions play a significant role in the AHP model when evaluating landslide susceptibility in large areas or when there is insufficient data on landslide locations to use statistical techniques. Therefore, the AHP model is still frequently utilized in numerous landslide studies worldwide.

5. Conclusion

Utilizing the AHP and combined AHP&FR methods, landslide susceptibility maps, and landslide hazard maps were prepared for the study area. They enable the identification of the highest landslide hazard areas and the prediction of future landslide sites. The AUC, SCAI, and P values were used to evaluate the performance of the models, which showed that both models could be used to assess landslide hazards in the study area. The findings indicated that the combined AHP&FR model is more accurate at predicting than the AHP model.

The AHP and combined AHP&FR models revealed that areas with high and very high hazards to landslides covered 37.5% and 40.56% of the study area, respectively. This indicates that the studied area is highly susceptible to landslides, which should be properly considered during disaster management, risk assessment, and land use planning. Finally, the methods presented in this research can be applied to landslide hazard assessments in other areas of Vietnam with similar landslide triggering factors.

Acknowledgement

This study is funded by the Institute of Geological Sciences – Vietnam Academy of Science and Technology in the national science and technology project under grant number ĐTĐL.CN-81/21.

Contributions of authors

Binh Van Duong, Igor Konstantinovich Fomenko, and Ha Viet Nhu – conceptualization, writing - original draft; Igor Konstantinovich Fomenko and Phuong Huy Nguyen - review & editing; Kien Trung Nguyen, Olga Nikolaevna Sirotkina and Ha Ngoc Thi Pham - contributed to the landslide susceptibility analysis, investigation.

References

Akgun, A., & Türk, N. (2010). Landslide susceptibility mapping for Ayvalik (Western Turkey) and its vicinity by multicriteria decision analysis. *Environmental Earth Sciences,* 61(3), 595-611. https://doi.org/10.1007/s12665-009-0373-1

Althuwaynee, O. F., Pradhan, B., & Lee, S. (2012). Application of an evidential belief function model in landslide susceptibility mapping. *Computers & Geosciences,* 44, 120-135. https://doi.org/10.1016/j.cageo.2012.03.003

Bui, T. D., Tran, A. T., Hoang, N.-D., Nguyen, Q. T., Nguyen, D. B., Ngo, V. L., & Pradhan, B. (2017). Spatial prediction of rainfall-induced landslides for the Lao Cai area (Vietnam) using a hybrid intelligent approach of least squares support vector machines inference model and artificial bee colony optimization. *Landslides,* 14(2), 447-458. https://doi.org/10.1007/s10346-016-0711-9

Bui, T. D., Tran, A. T., Klempe, H., Pradhan, B., & Revhaug, I. (2016). Spatial prediction models for shallow landslide hazards: a comparative assessment of the efficacy of support vector machines, artificial neural networks, kernel logistic regression, and logistic model tree. *Landslides,* 13(2), 361-378. https://doi.org/10.1007/s10346-015-0557-6

Cantarino, I., Carrion, M. A., Goerlich, F., & Martinez Ibañez, V. (2019). A ROC analysis-based classification method for landslide susceptibility maps. *Landslides,* 16(2), 265-282. https://doi.org/10.1007/s10346-018-1063-4

Dang, Q. T., Nguyen, D. H., Prakash, I., Jaafari, A., Nguyen, V. T., Phong, T. V., & Pham, B. T. (2020). GIS based frequency ratio method for landslide susceptibility mapping at Da Lat City, Lam Dong province, Vietnam. *Vietnam Journal of Earth Sciences,* 42(1), 55-66. https://doi.org/10.15625/0866-7187/42/1/14758

Dou, J., Yunus, A. P., Tien Bui, D., Sahana, M., Chen, C.-W., Zhu, Z., . . . Thai Pham, B. (2019). Evaluating GIS-Based Multiple Statistical Models and Data Mining for Earthquake and Rainfall-Induced Landslide Susceptibility Using the LiDAR DEM. *Remote Sensing,* 11(6), 638. https://doi.org/10.3390/rs11060638

Gholami, M., Ghachkanlu, E. N., Khosravi, K., & Pirasteh, S. (2019). Landslide prediction capability by comparison of frequency ratio, fuzzy gamma and landslide index method. *Journal of Earth System Science,* 128(2), 42.

https://doi.org/10.1007/s12040-018-1047-8

Greenbaum, D., Bowker, M., Dau, I., Dropsy, H., Greally, K., McDonald, A. J. W., . . . Tragheim, D. (1995a). Rapid methods of landslide hazard mapping : Fiji case study. *NERC*. Nottingham, UK. http://core.ac.uk/download/pdf/58059.pdf

Greenbaum, D., Tutton, M., Bowker, M., Browne, T., Buleka, J., Greally, K., . . . Tragheim, D. (1995b). Rapid methods of landslide hazard mapping : Papua New Guinea case study. *NERC*. Nottingham, UK. https://core.ac.uk/download/pdf/57306.pdf

Le, T. T. T., Tran, T. V., Hoang, V. H., Bui, V. T., Bui, T. K. T., & Nguyen, H. P. (2021). Developing a Landslide Susceptibility Map Using the Analytic Hierarchical Process in Ta Van and Hau Thao Communes, Sapa, Vietnam. *Journal of Disaster Research,* 16(4), 529-538. https://doi.org/10.20965/jdr.2021.p0529

Ma, Z., Mei, G., & Piccialli, F. (2021). Machine learning for landslides prevention: a survey. *Neural Computing and Applications,* 33(17), 10881-10907. https://doi.org/10.1007/s00521-020-05529-8

Mandal, S., & Mondal, S. (2019). Statistical Approaches for Landslide Susceptibility Assessment and Prediction. *Springer International Publishing*. Switzerland, 200 pages.

Mokarram, M., & Zarei, A. R. (2018). Landslide Susceptibility Mapping Using Fuzzy-AHP. *Geotechnical and Geological Engineering,* 36(6), 3931-3943. https://doi.org/10.1007/s10706-018-0583-y

Mokhtari, M., & Abedian, S. (2019). Spatial prediction of landslide susceptibility in Taleghan basin, Iran. *Stochastic Environmental Research and Risk Assessment,* 33(7), 1297-1325. https://doi.org/10.1007/s00477-019-01696-w

Nguyen, T. K., Tran, T. V., Vy, T. H. L., Pham, L. H. L., & Nguyen, Q. T. (2021). Landslide Susceptibility Mapping Based on the Combination of Bivariate Statistics and Modified Analytic Hierarchy Process Methods: A Case Study of Tinh Tuc Town, Nguyen Binh District, Cao Bang Province, Vietnam. *Journal of Disaster Research,* 16(4), 521-528. https://doi.org/10.20965/jdr.2021.p0521

Nguyen, V. C., & Dao, V. T. (2007). Investigation and research of landslide geohazard in north-western part of Vietnam for the sustainable development of the territory. In. Annual Report of FY 2006, The Core University Program between Japan Society for the Promotion of Science (JSPS) and Vietnamese Academy of Science and Technology (VAST). *Osaka University*. Osaka. 269-280.

Pourghasemi, H. R., Jirandeh, A. G., Pradhan, B., Xu, C., & Gokceoglu, C. (2013). Landslide susceptibility mapping using support vector machine and GIS at the Golestan Province, Iran. *Journal of Earth System Science,* 122(2), 349-369. https://doi.org/10.1007/s12040-013-0282-2

Saaty, T. L. (1977). A scaling method for priorities in hierarchical structures. *Journal of Mathematical Psychology,* 15(3), 234-281. https://doi.org/10.1016/0022-2496(77)90033-5

Saaty, T. L. (1990). How to make a decision: The analytic hierarchy process. *European Journal of Operational Research,* 48(1), 9-26. https://doi.org/10.1016/0377-2217(90)90057-I

Saaty, T. L. (2002). Decision Making with the Analytic Hierarchy Process. *Scientia Iranica,* 9(3), 215-229. http://scientiairanica.sharif.edu/article_2696.html

Saaty, T. L. (2008). Decision making with the Analytic Hierarchy Process. *Int. J. Services Sciences Int. J. Services Sciences,* 1, 83-98. https://doi.org/10.1504/IJSSCI.2008.017590

Saaty, T. L., & Vargas, L. (2001). Models, Methods, Concepts & Applications of the Analytic Hierarchy Process. *Springer US*. New York, 333 pages.

Senouci, R., Taibi, N.-E., Teodoro, A. C., Duarte, L., Mansour, H., & Yahia Meddah, R. (2021). GIS-Based Expert Knowledge for Landslide Susceptibility Mapping (LSM): Case of Mostaganem Coast District, West of Algeria. *Sustainability,* 13(2). https://doi.org/10.3390/su13020630

Shano, L., Raghuvanshi, T. K., & Meten, M. (2020). Landslide susceptibility evaluation and hazard zonation techniques – a review. *Geoenvironmental Disasters,* 7(1), 18. https://doi.org/10.1186/s40677-020-00152-0

Shano, L., Raghuvanshi, T. K., & Meten, M. (2021). Landslide susceptibility mapping using frequency ratio model: the case of Gamo highland, South Ethiopia. *Arabian Journal of Geosciences,* 14(7), 623. https://doi.org/10.1007/s12517-021-06995-7

Šimundić, A.-M. (2009). Measures of Diagnostic Accuracy: Basic Definitions. *EJIFCC,* 19(4), 203-211. https://pubmed.ncbi.nlm.nih.gov/27683318

Süzen, M. L., & Doyuran, V. (2004). A comparison of the GIS based landslide susceptibility assessment methods: multivariate versus bivariate. *Environmental Geology,* 45(5), 665-679. https://doi.org/10.1007/s00254-003-0917-8

Tran, T. V., Alkema, D., & Hack, R. (2019). Weathering and deterioration of geotechnical properties in time of groundmasses in a tropical climate. *Engineering Geology,* 260, 105221. https://doi.org/10.1016/j.enggeo.2019.105221

Tran, T. V., Alvioli, M., & Hoang, V. H. (2021). Description of a complex, rainfall-induced landslide within a multi-stage three-dimensional model. *Natural Hazards*. https://doi.org/10.1007/s11069-021-05020-0

Vahidnia, M. H., Alesheikh, A. A., Alimohammadi, A., & Hosseinali, F. (2009). Landslide Hazard Zonation Using Quantitative Methods in GIS. *IJCE,* 7(3), 176-189. http://ijce.iust.ac.ir/article-1-289-en.html

Varnes, D. J. (1978). Slope Movement Types and Processes. In Robert L Schuster & Raymond J Krizek (Eds.). Landslides: Analysis and Control. Special Report 176. *Transportation Research Board, National Academy of Sciences*. Washington. 11-33. http://onlinepubs.trb.org/Onlinepubs/sr/sr176/176-002.pdf

Varnes, D. J., International Association of Engineering Geology, & Commission on Landslides and Other Mass Movements on Slopes, (1984). Landslide hazard zonation a review of principles and practice. *Unesco*. Paris, 63 pages.

Yalcin, A., Reis, S., Aydinoglu, A. C., & Yomralioglu, T. (2011). A GIS-based comparative study of frequency ratio, analytical hierarchy process, bivariate statistics and logistics regression methods for landslide susceptibility mapping in Trabzon, NE Turkey. *CATENA,* 85(3), 274-287. https://doi.org/10.1016/j.catena.2011.01.014

Zhang, G., Cai, Y., Zheng, Z., Zhen, J., Liu, Y., & Huang, K. (2016). Integration of the Statistical Index Method and the Analytic Hierarchy Process technique for the assessment of landslide susceptibility in Huizhou, China. *CATENA,* 142, 233-244. https://doi.org/10.1016/j.catena.2016.03.028.